# An Insight into Water and Temperature Management in Unitised Regenerative Fuel Cell (URFC) during Mode Change

Ahmad Adam Danial Shahril<sup>a</sup>, CT Aisyah Sarjuni<sup>a</sup>, Edy Herianto Majlan<sup>a</sup>, Mohd Shahbudin Mastar<sup>a,b</sup>, Abu Bakar Sulong<sup>a,b</sup>, Bee Huah Lim<sup>a\*</sup>

<sup>a</sup> Fuel Cell Institute, Universiti Kebangsaan Malaysia, 43600 Bangi, Selangor, Malaysia <sup>b</sup>Faculty of Engineering and Built Environment, Universiti Kebangsaan Malaysia, 43600 Bangi, Selangor, Malaysia

#### Abstract

Although water-related issues are no stranger to conventional fuel cells, unitised regenerative fuel cells (URFC) sustain amplified effects from this condition due to their transition states. Fuel cell (FC) mode start-ups post water electrolyser (WE) operations suffer significantly due to flooding. Past studies validated the significance of water and heat distribution towards the dynamic response of URFC. Due to complications involved in the numerical study of mode change conditions, this paper suggests the basic procedures required for numerical analysis of the WE to FC mode conversion in a URFC where the final result of each mode is taken as the initial result for the next one. Water removal through gas purging is currently one of the best methods to reduce transient time and increase FC start-up efficiency. However, crucial purging conditions such as operating current density, temperature and purging period play an important role in the successful transition. Lower operating current density, ranging below 0.02A/cm<sup>2</sup> is reported to have a smoother transition compared to current density above 0.12A/cm<sup>2</sup>. Gas purge relative humidity is only effective up to 4% at the anode and poses no effect during a severe flooding condition. Furthermore, the temperature has the lowest response towards the cell heat source, increasing the transient period. The cell experiences high WE mode efficiency at 80°C, but it suffers significant catalytic loss. The insight will provide a more profound comprehension of water management during WE mode and a suitable administrative method to achieve smooth FC start-ups.

**Keywords:** Unitised regenerative fuel cell, Mode transition, Water electrolyser, Computational Fluid Dynamics.

#### 1. Introduction

Amidst the ever-expanding technological innovation, environmental consciousness concurrently grows towards an ultimate sustainable ambition. The advancement in fuel cell technologies leads to a steady increase in the reliance on hydrogen as an energy source for renewable energies. One of the most common challenges for renewable energies is their intermittent nature. Hence, a practical and consistent technology is required to produce clean energy without interruption [1,2]. A cost-effective energy-storage and production device termed a unitised regenerative fuel cell (URFC) can be adapted to counteract these irregularities. A URFC is a device that can perform both the functions of a discrete

\* Corresponding author. Tel.: +603-8911 8529; fax: +603-8911 8530 E-mail address: beehuah@ukm.edu.my

Manuscript History:

Received 23 April, 2025, Revised 4 June, 2025, Accepted 6 June, 2025, Published 31 October, 2025 Copyright © 2025 UNIMAS Publisher. This is an open access article under the CC BY-NC-SA 4.0 license. https://doi.org/10.33736/jaspe.9535.2025



fuel cell and a water electrolyser under one unitised system as shown in Figure 1[3]. The additional transient states of this device also translate to a more complicated dynamic response where water and temperature-related issues concerning mode changes are critical [4]. Maintaining an optimal hydration environment is complicated for a URFC, especially during mode changes, particularly from water electrolyser (WE) mode to fuel cell (FC) mode conversion. Therefore, understanding the significance of mode conversions towards water distribution can preserve the cyclic efficiency and lifespan of a URFC. Water is understood to behave differently during both FC and WE modes. FC mode start-up is more complicated after WE operation due to residual water flooding the oxygen side electrodes. Water removal ensures a smooth operation and start-up of FC [5]. Hence, various reports have shown that residual water removal promotes mass transfer, leading to a smoother FC start-up. Past studies have proposed several methods to direct water content, such as inlet relative humidity, gas purging, and current density [6-8]. Excessive water removal leads to overpotential concentration and potential local hotspots at the electrodes. With an interest in fuel cell technology, extended study is always recommended to considerably reduce water and temperature-related issues to achieve highly feasible cyclic efficiency and a more durable cell. Therefore, this paper will provide a short insight into the significance of WE to FC mode conversion and how it will affect the dynamic response of a URFC, leading to an overall performance increase.

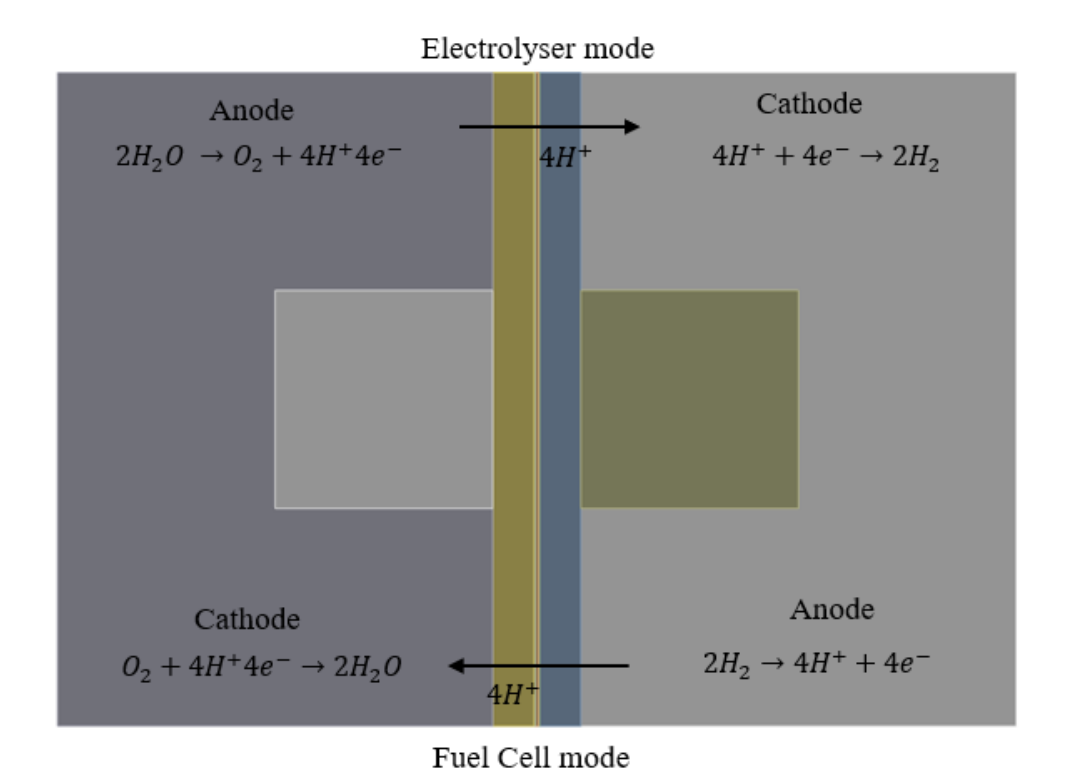


Figure 1. Schematic of a URFC at electrolyser and fuel cell mode.

### 2. Unitised regenerative mode change

### 2.1. Water electrolyser mode operation

The WE mode of a URFC displays the regeneration of gaseous hydrogen and oxygen by the water splitting process. Theoretically, the current direction is changed during the phase where the

Jaurnal of Applied Science SPE JASP Process Engineering

polarity of the electrodes is reversed. The equations for water splitting are shown in equations (1) to (3).

Anode: 
$$2H_2O \to O_2 + 4H^+4e^-$$
 (1)  
Cathode:  $4H^+ + 4e^- \to 2H_2$  (2)

Cathode: 
$$4H^+ + 4e^- \rightarrow 2H_2$$
 (2)

Overall equation: External energy 
$$+ 2H_2O \rightarrow 2H_2 + O_2$$
 (3)

Unlike FC, WE mode demands external energy. In most cases, it is the electrical energy that initiates the electrolysis process, where hydrogen gas is generated. The accommodation for oxygen evolution reaction (OER) during water electrolysis presents durability issues of electrocatalysts [9], which disrupt the proceedings of FC operation. However, if fuel starvation had been avoided, the post-FC operation would not be much of an issue for a WE mode start-up. A study reported that regardless of FC current density and water production, the values are not sufficient to initiate and sustain electrolysis operation for WE mode [10]. Therefore, a delayed water supply during WE mode start-up causes a voltage overshoot that might permanently damage secondary equipment such as the peristaltic pumps [11]. During WE mode operation, flooding and dehydration are the most common issues that disrupt its proceedings. Klose et al. [12] showed that flooding is mitigated by reducing 4% of anode's relative humidity. Correspondingly, Immerz et al. [13] revealed that dehydration of the anode electrode would reduce protonic conductivity, thus reducing WE mode performance. Unlike FC, where the start-up procedure and operation are highly affected by residual water from WE mode operation, WE mode is primarily sensitive to the supplied water and not the prior operation of FC.

#### 2.2. URFC modelling

Generally, FC can be modelled in numerical analysis using a zero, one, two, or threedimensional model. Aubras et al. [14] showed the significance of using a dimensionless proton exchange membrane (PEM) water electrolyser model. They showed that the dimensionless model provides large amounts of data for hierarchical learning due to a speedier computing period. Additionally, the performance of the PEM water electrolyser is assessed through the Wagner number, which determines the membrane dehydration condition. Guarnieri et al. [15] reported that dimensionless fuel cell models are often adapted with the intention of performance forecasting through numerical optimisation. Dimensionless models often exhibit preliminary-based results despite the low computational time. Chandesris et al. [16] adopted a one-dimensional model for a PEM water electrolyser where the domains from zero-dimensional models are connected to the appropriate boundary conditions. This model revealed that the degradation that primarily occurs at the hydrogen side of the electrode is primarily due to operational temperature. Springer et al. [17], in their onedimensional PEM fuel cell model, demonstrated that using a thinner membrane reduced the overall cell resistance. However, complex values such as heat flux or inlet humidification are one of its many constraints. Regarding modelling mode changes, the multi-physics mathematical model is usually opted for and typically achieved through a two or three-dimensional model.

Xiao et al. [18], in their two-dimensional URFC model, showed the transient response during mode change procedures where various heat generations such as Joule heat, reaction heat and heat through activation polarisation are considered. They revealed that the resulting overall temperature is the highest at the membrane during WE mode operation and is exothermic for both modes. Similarly, Wang et al. [19] set a two-dimensional URFC model to analyse operating parameter distribution during mode changes. The operating parameters of hydrogen, oxygen, water mass fraction, and electrolyte potential have all responded to the jump in voltage through mode change. Another study that adopted the two-dimensional URFC model revealed that the transient response of gas mass fraction in the flow channel, gas diffusion layer and catalyst layer showed a delay of roughly 0.2s upon mode changes relative to the operating voltage [20]. The fuel cell start-ups and shutdowns are expected in a conventional fuel cell, and a URFC considers WE mode start-ups and shutdowns and gas purging procedures. Mode switching is of great significance towards the performance of a URFC [4], and careful measures are adopted to prevent cell failure. Typically, these procedures are done through

Journal of Applied Science

simulation software to be economically feasible. A more accurate representation of the cell would be a complete three-dimensional model. Specific steps are required to account for the mode change. Three solving procedures were introduced for a three-dimensional, mode-changing model of a URFC [21] [22]. They are the steady-steady WE mode, transient gas purging (GP) period and transient FC mode operation.

The modeling WE to FC mode for a URFC is to perform a steady state WE mode operation to obtain the distributions and generations of reactants and products. The initial condition for the transient GP period is calculated from the WE mode operation results. Similarly, the initial condition for transient FC mode operation is adopted from the final results of the calculated GP period [21]. Prior to these procedures, a three-dimensional geometry or computational domain of the URFC cell is modelled, where the meshing and boundary distributions are justified. The geometrical design of the URFC shown in Figure 2 includes the bipolar plate (BPP) as the current collector, anode and cathode inlet channel for reactant or product transport, gas diffusion layer (GDL) of two-phase species, catalyst layer (CL) for reactions and proton-exchange membrane (PEM) for proton transport. During the WE mode operation, liquid water enters the anode inlet, and water splitting occurs at the anode catalyst layer [21]. Liquid water splits into hydrogen protons, electrons, and oxygen as stated in equation 1. The hydrogen proton permeates through the membrane, and electrons flow through the external circuit at the cathode to form hydrogen [23]. Additionally, the external circuit is switched off during the transition of WE to FC mode for gas purging (GP) process to prepare for the FC mode condition [24]. During the gas purging process, hydrogen and oxygen reactants are supplied into the anode and cathode to remove residual water along the flow channel during the operation of WE. FC mode is an inverted process of WE, whereby water is produced as a byproduct. As the mode changes, the current flow direction is changed to allow for the change in polarity that accommodates FC mode operation [21]. Table 1 shows the symbols assigned to denote the geometrical parameters in Figure 2.

Table 1. URFC geometry parameters.

Symbols	Parameters (mm)	
$W_{\mathrm{BP}}$	Bipolar plate width	
$W_{rib}$	Rib width	
Wch	Channel width	
$H_{BP}$	Bipolar plate height	
H <sub>ch</sub>	Channel height	
$\delta_{ m GDL}$	GDL thickness	
$\delta_{ m cl}$	CL thickness	
$\delta_{ m mem}$	Membrane thickness	
$L_{\mathrm{BP}}$	Bipolar plate length	



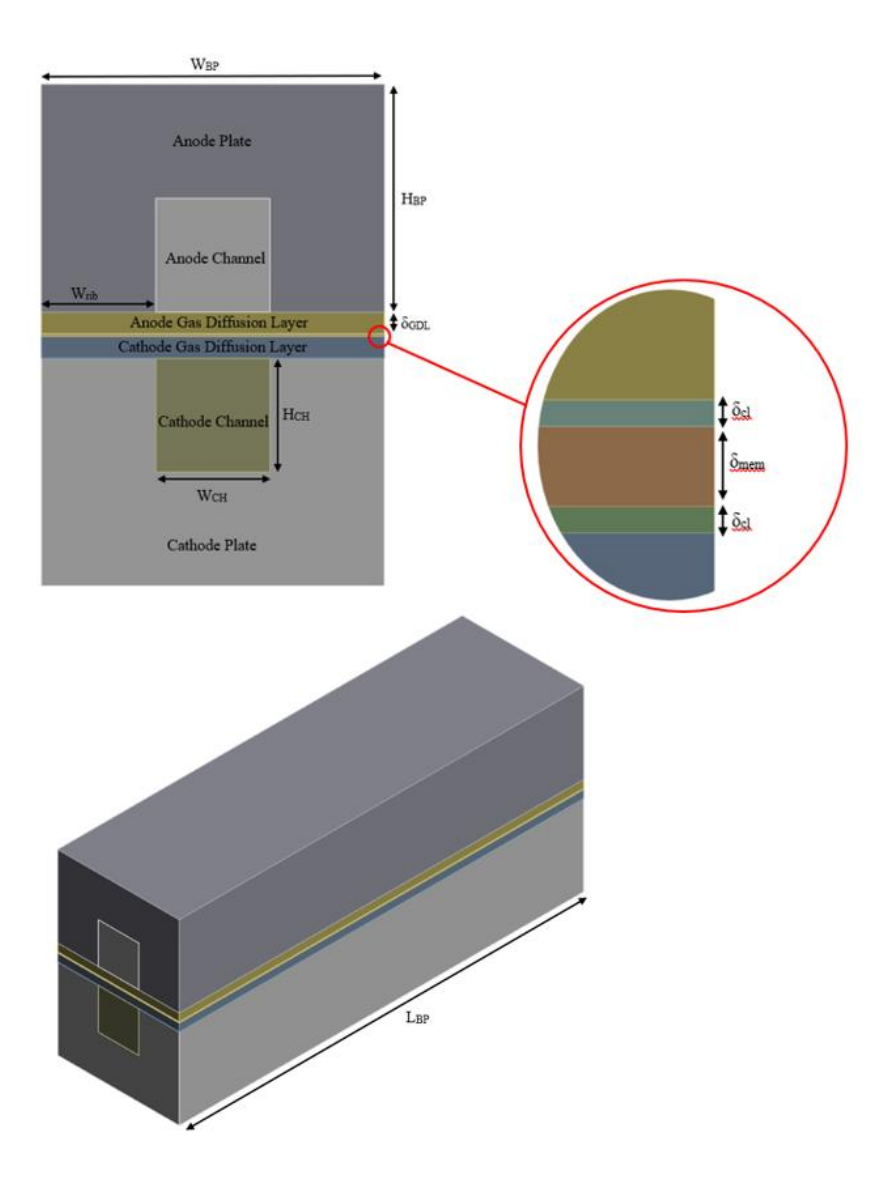


Figure 2. Geometry of a single-channel URFC.

In most cases where modelling is involved for fuel cells, a single-channel model is commonly opted for during the early phase of study [25, 26]. This is mainly due to the simplicity of the contact surface area regardless of the flow field pattern, as shown in Figure 3. A minimal discretised number of mesh is determined through a grid independence test (GIT), to obtain optimal results [28][29], and the optimal results are plotted in a polarisation curve for either WE or FC [27].



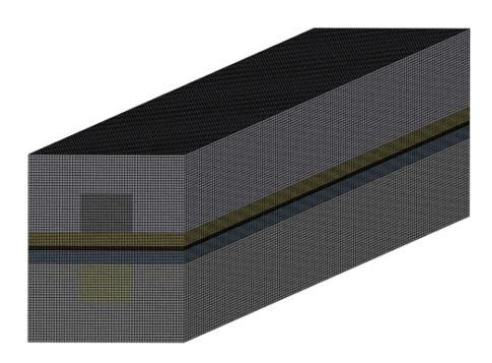


Figure 3. Meshing of a single-channel URFC.

For a 3D URFC model, the general assumptions to solve the governing equations include:

- a) Gas is assumed to be an ideal gas [21][30];
- b) Gas flow is laminar, fully developed and incompressible [19][21][31][18];
- c) PEM is impermeable to reactant gases [21][32];
- d) Porous layers are isotropic and homogeneous [21] [33]

These assumptions are made subjectively to the study area and are relative to the study objectives. Collective governing equations applicable in the mass transport and energy transport of WE and FC are tabulated in Table 2.

The conservation of mass and momentum equation (as shown in equations (4) and (5)) and the remarkable conservation of two-species mixtures (equation (8)) are applied for gas transport analysis. The model adopted for analysis is assumed to be a closed system where the mass flowing in is required to equal the mass flowing out. Equations (7) and (8) apply the mass equation and Darcy's law, respectively, for the transport of dissolved water to define fluid flow through the porous medium. The Nernst-Planck equation is a mass conservation equation used to demonstrate the movement of charged species in a fluid medium (equation (9)). Similarly, the energy conservation equation shown in equation (10) describes that the total energy in an isolated system is constant. Energy losses through heat for the URFC model are neglected due to the system's low operational temperature. URFC operational temperature is typically regulated between 20 - 90°C [39]. Determining equations will lead to higher accuracy and better visualisation of how the parameters behave relative to each other. Since electrochemical reaction occurs at the catalyst layer of both anode and cathode, current charges are also generated and consumed in these layers. Butler-Volmer equation (11) is applied to express the electrochemical reaction rate at these catalyst layers [21]. Nernst equation (12) is applied to express the equilibrium potential of the oxygen catalyst layer, as the influence of reactant partial pressure is negligible for numerical analysis.

Jaurnal of Applied Science

Table 2. URFC numerical governing equations.

Transport	Governing Equations	
Transport of gaseous	Mass conservation [31]	
mixture	$\frac{\partial \left(\varepsilon^{eff}\rho_g\right)}{\partial t} + \nabla(\rho_g u_g) = S_m$	(4)
	Momentum conservation [34]	(5)
	$\begin{split} \frac{\rho_g}{\varepsilon^{eff}} \left( \frac{\partial u_g}{\partial t} + (u_g \cdot \nabla) (\frac{u_g}{\varepsilon^{eff}}) \right) \\ &= \nabla \cdot \left\{ -p_g I + (\frac{\mu_g}{\varepsilon^{eff}}) \left[ \nabla u_g + (\nabla u_g)^T \right] - \frac{2}{3} (\frac{\mu_g}{\varepsilon^{eff}}) (\nabla \cdot u_g) I \right\} - \left( \frac{\mu_g}{\kappa_0 \kappa_{rg}} + \frac{1}{(\varepsilon^{eff})} (\nabla \cdot u_g) I \right) \end{split}$	$\frac{S_m}{S_{eff})^2}$ ) $u_g$
	Special conservation for a two-species mixture [35]	
	$\frac{\partial c_i}{\partial t} + \nabla \cdot (-D^{eff} \nabla c_i) + \nabla \cdot (c_i u_g) = S_i$	(6)
Liquid water transportation	Mass equation for liquid phase [36]	
transportation	$\frac{\partial(\varepsilon_0\rho_1)}{\partial t} + \nabla(\rho_1u_1) = S_{V1}$	(7)
	Darcy's law [21]	
	$-\nabla p_1 = \frac{\mu_1}{\kappa_0 \kappa_{r1}} \ u_1$	(8)
Transport of	Nernst-Planck equation [21]	
dissolved water	$\frac{\rho_{mem}}{EW}\frac{\partial}{\partial t}(\alpha_{mem}\lambda) + \frac{\rho_{mem}}{EW}\nabla(-D_{mw}^{eff}\nabla\lambda) + \nabla\left(\frac{2.5}{22F}i_{mem}\lambda\right) = S_{mw}$	(9)
Energy transfer	Energy conservation equation [21]	
	$\frac{\partial}{\partial t} \left( \sum (\varepsilon_j \rho_j C_{p,j}) T \right) + \sum (\varepsilon_j \rho_j C_{p,j} u_j) \cdot \nabla T + \left( -k_{eff} \nabla T \right) = S_T$	(10)
Charge transfer	Butler-Volmer equation [37]	
	$i_{v} = \alpha_{v,i} i_{0,i}^{ref} \left[ \exp\left(\frac{a_{a} F \eta}{RT}\right) - \exp\left(-\frac{a_{c} F \eta}{RT}\right) \right]$	(11)
	Nerst equation [38]	
	$E^{eq} = 1.229 - 9.0 \times 10^{-4} (T - 298.15)$	(12)

Jaurnal of Applied Science JA PE
JA Process Engineering

# 3. Transient response

## 3.1. Water management

Water plays a critical role in the stability of URFC. FC and WE modes' electrochemical process and performance are fundamentally associated with water transport [40]. During WE mode, waterrelated issues are partly due to oxygen evolution reaction (OER) and hydrogen evolution reaction (HER) [41]. The cell risks flooding without proper regulations since water is the reactant for the WE mode. Klose et al. [12] showed that a minor change in relative humidity could increase the risk of cell flooding. Different approaches are taken to counter flooding under a high WE mode current density. Oxygen side porous layers' porosity at high current density conditions is critical for adequate water removal [42]. Cruz et al. [43] opted for the use of modified titanium porous GDL to improve fluid distribution and electrical conduction during WE mode operation. Fornaciari et al. [44] studied with a mathematical model and reported that using a vapour-fed inlet reduces the cell's hydration value, indicating the possibility of dehydration during WE mode operation. Immerz et al. [13] showed that if water stoichiometric value is less than 5, dehydration is likely to occur at the anode catalyst layer and membrane. The occurrence of dehydration during WE mode operation is low compared to cell flooding. During mode change, reactant switching will significantly affect electrochemical reactions [11]. Guo et al. [21], in their three-dimensional URFC model, showed that residual water at the membrane region would cause FC start-up failure due to mass transport limitation.

One of the few methods to manage water content during mode change is GP. Ito et al. [24] 's study reveals that high frequency resistance (HFR) indicates the membrane humidification. They reported that membrane humidification initially increased and rapidly dropped through gas purging. Pre-switching procedure of GP is also an effective method to remove residual water. Guo et al. [22] reported that the water volume fraction within the porous layers decreased from 0.88 to 0.50 in just one second. The effectiveness of the rest of the water will require a longer GP period. On the other hand, Yuan et al. [45] suggested that a high GP flow rate is more desirable than a long GP period. They further elaborate that an FC start-up at a current density of 1A cm<sup>-2</sup> requires an extended GP time. Under normal operating conditions, a lengthy GP would risk creating the membrane dehydration phenomenon. A prolonged dehydration phenomenon would lead to voltage undershoot and eventually cause a start-up failure on FC [46]. On a condition of constant loading, the GP process is highly dependent on the FC current density. In their experiment, Liu et al. [47] studied the dynamic effects of water during FC start-up. They concluded that a low FC current density would lead to an optimal start-up condition where temperature elevates at a higher current density and causes local hotspots. In contrast, inefficient heat removal retards mode start-up.

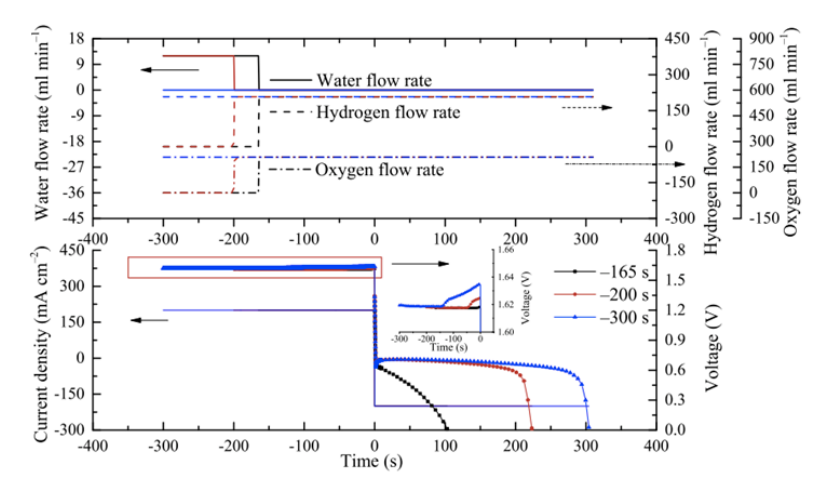


Figure 3. FC start-up at multi-reactant and current switch time gap [48].

Jaurnal of Applied Science PE JA Process Engineering

Residual water before FC start-up is also removed by increasing the time interval between the reactant and current switch. Yuan et al. [48] revealed that water is removed through electrolysis during a long time gap, increasing concentration overpotentially. Figure 3 shows that at a 300-second interval, concentration overpotential is at its maximum value of 1.63 V. A high FC current density could cause water starvation, damaging the membrane. Water starvation leads to other temperature-related issues, as both variables affect one another.

Water management is a crucial parameter for a stable mode change operation of a URFC. WE mode operation often suffers from water flooding due to the slow removal of water. Water in the cell is typically managed through the GP process during mode change to avoid the FC start-up failure. A sufficient time interval between reactant and current change also aids FC start-up, providing additional time for residual water removal. In a nutshell, a higher flow rate of GP would result in a positive environment compared to a longer purging process. Excessive water removal during the GP would increase the cell's concentration overpotential and elevate the cell temperature. The effects of temperature on URFC cells will be discussed in the next section.

#### 3.2. Temperature management

URFC experiences greater overall degradation than a conventional fuel cell due to its additional transient states. Literature has reported that the lifespan of a URFC is about 600 hours [49], and conventional fuel cells are registered to achieve a lifespan of 5,000 to 20,000 hours [50]. Besides water management, the temperature of URFC is another major factor contributing to cell degradation. The operating temperature for a URFC system is between 20°C and 90°C [39]. The water removal rate will be more efficient at an elevated temperature, but there is a risk of membrane dehydration. In their experiment, Shin et al. [51] justified that the hydrogen discharge rate increases with temperature and current density. Conversely, a study by Wang et al. [52] reveals that temperature non-uniformity increases with current density. The condition appears at a low saturation value, where localised hotspots are likely to occur and damage the cell. During mode change, the temperature is also susceptible to changes. A study has revealed that the temperature has a slower response to the cell heat source than current density [53].

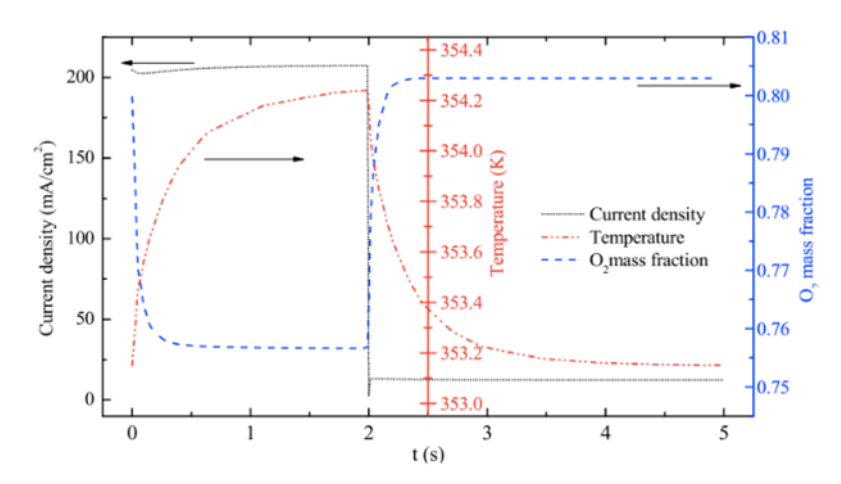


Figure 4. Temperature and current density response from WE to FC mode conversion[15]

The temperature profile was reported to have a relatively slower response than the current density. Figure 4 shows an instant current density response due to the heat source during WE mode to FC conversion. Additionally, the heat transfer process was also seen to have increased the transient response time [54]. Guo et al. [31], on the other hand, reported that the average cell temperature is

Journal of Applied Science PE JA Process Engineering

always higher than its initial temperature, regardless of the operational modes. The study from Liu et al. [55] shows that reactant switching decreases the cell temperature during WE start-up due to low-temperature water but increases with operation. Additionally, heat fluxes drastically reduce at both electrodes during mode change due to reversible electrochemical reactions and a reduction in current density [56].

Table 3. Percentage of catalyst loss at different operating temperatures [57]

Catalyst	Percenta	Percentage Lost	
·	30°C	60°C	
Platinum	$48.3 \pm 6.0$	$65.8 \pm 3.5$	
Iridium	$54.0 \pm 10.0$	$54.3 \pm 1.5$	

Besides a slow response time, the significance of temperature could also be observed through physical degradation. Table 3 shows the percentage loss at two operating temperatures after three cycles of URFC mode change. Catalytic loss accelerates with the operation of WE mode due to the oxygen evolution reaction (OER) and worsens at an elevated temperature. Additionally, it promotes the oxidation of the carbon-based catalyst support at high temperatures. Theoretically, the loss of the electrochemical surface during cell start-up depends on the carbon support [58]. This further determines that a high FC current density during start-up could potentially harm the membrane due to temperature elevation. A study by Regmi et al. [59] achieved a 60% round-trip efficiency with an average operating temperature of 80°C. They used the Pt-black and Ir-black bifunctional catalyst layers to obtain a high-performance result. The Pt-black is sufficient to maintain a hydrogen oxidation reaction that improves FC performance, and the Ir-black reduces performance loss during WE operation. Therefore, catalyst material selection is crucial during the operation of FC at high current density.

Thus, both temperature management and water management are crucial for URFC. Both factors play an important role in cell degradation. Metallic-based catalysts typically reduce the temperature response period towards the cell's heat source. WE mode operations are efficient under a higher operating temperature. However, once it exceeds the optimum temperature, the cell will be more vulnerable to irreversible damage, such as catalyst degradation.

### 4. Conclusion

URFCs are taking the fuel cell and electrolyser device, showing potential for clean energy generation. This paper provides insight into the possibilities of employing numerical methods to address the challenges for the development of URFC. The advantage of URFC is a single device with dual functions in generating clean energy, which could replace the conventional fuel cells and electrolysers that generally reduce the cost of hydrogen energy. The major hurdle in URFC design occurs during cell transition conditions, commonly referred to as the mode change effect. The effect of mode change, specifically from WE to FC mode, on the dynamics of a URFC significantly impacts the water and temperature management during the cell operation. Managing these conditions during mode changes is crucial as it impacts the cyclic efficiency and lifespan.

In conclusion, URFCs experience significant challenges during the mode change from WE to FC, primarily due to residual water from the WE stage causing flooding and hindering efficient FC start-up. While gas purging is commonly employed for water removal, excessively long purges can lead to membrane dehydration and voltage undershoot. Transitioning between WE and FC mode commonly fails due to flooding, as water remains in flow channels and gas diffusion layers, which consequently hinders the mass transport of reactant during FC mode. The common method employed is gas purging using nitrogen gas, followed by hydrogen-oxygen gas towards the flow channel for a sufficient time. However, excessive purging could lead to membrane dehydration and voltage overshoot; vice versa, insufficient purging causes flooding. Thus, further investigation is required to

obtain the optimal purging and operating conditions for a smooth transition between WE and FC mode.

Operating temperatures of a URFC range between 20°C and 90°C. This plays a crucial role in balancing the water content in cells, where higher temperatures improve the WE efficiency. However, it accelerates catalytic loss, particularly platinum, and promotes carbon support oxidation. This significantly shortens the lifespan of URFCs to below 600 hours compared to conventional fuel cells, which could achieve up to 20,000 hours. Thus, improvement of operating temperature to improve the efficiency and lifespan is required, and possibly employing numerical methods for optimal URFC operating criteria.

## Acknowledgements

The authors acknowledge the support from the Ministry of Higher Education (MOHE), Malaysia, through grant no. HICOE-2023-005 and TRGS/1/2022/UKM/01/8/1 for the research opportunity.

#### **Conflict of Interest**

We declare no conflict regarding the publication of the study.

### References

- [1] Becker, S., Frew, B. A., Andresen, G. B., Zeyer, T., Schramm, S., Greiner, M., & Jacobson, M. Z. (2014). Features of a fully renewable US electricity system: Optimised mixes of wind and solar PV and transmission grid extensions. *Energy*, 72, 443–458. <a href="https://doi.org/10.1016/j.energy.2014.05.067">https://doi.org/10.1016/j.energy.2014.05.067</a>
- [2] Weitemeyer, S., Kleinhans, D., Vogt, T., & Agert, C. (2015). Integration of Renewable Energy Sources in future power systems: The role of storage. *Renewable Energy*, 75, 14–20. https://doi.org/10.1016/j.renene.2014.09.028
- [3] Gabbasa, M., Sopian, K., Fudholi, A., & Asim, N. (2014). A review of unitised regenerative fuel cell stack: Material, design and research achievements. *International Journal of Hydrogen Energy*, *39*(31), 17765–17778. <a href="https://doi.org/10.1016/j.ijhydene.2014.08.121">https://doi.org/10.1016/j.ijhydene.2014.08.121</a>
- [4] Vincent, I., Lee, E., & Kim, H. (2020). Solutions to the water flooding problem for unitised regenerative fuel cells: status and perspectives. *RSC Advances*, 16844–16860. <a href="https://doi.org/10.1039/d0ra00434k">https://doi.org/10.1039/d0ra00434k</a>
- [5] Guo, H., Guo, Q., Ye, F., Ma, C. F., Liao, Q., & Zhu, X. (2019). Improving the electric performance of a unitised regenerative fuel cell during mode switching through mass transfer enhancement. *Energy Conversion and Management*, 188, 27–39. https://doi.org/10.1016/j.enconman.2019.03.033
- [6] Guo, Q., Guo, H., Ye, F., & Ma, C. F. (2023). Experimental and numerical studies of mode switching performance and water transfer in unitized regenerative fuel cells with different channel structures. *Energy Conversion and Management*, 280. <a href="https://doi.org/10.1016/j.enconman.2023.116810">https://doi.org/10.1016/j.enconman.2023.116810</a>
- [7] Tran, M., & Demuren, A. (2025). Thermal management for optimal performance of polymer electrolyte membrane unitized regenerative fuel cells. *Next Energy*, 8, 100271. <a href="https://doi.org/10.1016/j.nxener.2025.100271">https://doi.org/10.1016/j.nxener.2025.100271</a>
- [8] Chen, W., Meng, K., Luo, Z., Deng, Q., Zhang, N., Chen, K., & Chen, B. (2025). Segmented current diagnostics for mode switching and fuel cell mode startup behavior in unitized regenerative proton exchange membrane fuel cells. Energy Conversion and Management, 336, 119894. https://doi.org/10.1016/j.enconman.2025.119894
- [9] Reier, T., Oezaslan, M., & Strasser, P. (2012). Electrocatalytic oxygen evolution reaction (OER) on Ru, Ir, and pt catalysts: A comparative study of nanoparticles and bulk materials. *ACS Catalysis*, *2*(8), 1765–1772. <a href="https://doi.org/10.1021/cs3003098">https://doi.org/10.1021/cs3003098</a>
- [10] Yan Li, H., Guo, H., Ye, F., & Fang Ma, C. (2018). Experimental investigation on voltage response to operation parameters of a unitised regenerative fuel cell during mode switching from fuel cell to

120

Journal of Applied Science

- electrolysis cell. *International Journal of Energy Research*, 42(10), 3378–3389. https://doi.org/10.1002/er.4073
- [11] Yuan, X. M., Ye, F., Liu, J. X., Guo, H., & Ma, C. F. (2019). Voltage response and two-phase flow during mode switching from fuel cell to water electrolyser in a unitised regenerative fuel cell. *International Journal of Hydrogen Energy*, 44(30), 15917–15925. https://doi.org/10.1016/j.ijhydene.2018.07.017
- [12] Klose, C., Saatkamp, T., Münchinger, A., Bohn, L., Titvinidze, G., Breitwieser, M., Kreuer, K. D., & Vierrath, S. (2020). All-Hydrocarbon MEA for PEM water electrolysis combining low hydrogen crossover and high efficiency. *Advanced Energy Materials*, 10(14), 1–9. <a href="https://doi.org/10.1002/aenm.201903995">https://doi.org/10.1002/aenm.201903995</a>
- [13] Immerz, C., Bensmann, B., Trinke, P., Suermann, M., & Hanke-Rauschenbach, R. (2018). Local current density and electrochemical impedance measurements within 50 cm single-channel PEM electrolysis cell. *Journal of The Electrochemical Society*, 165(16), F1292–F1299. https://doi.org/10.1149/2.0411816jes
- [14] Aubras, F., Rhandi, M., Deseure, J., Kadjo, A. J. J., Bessafi, M., Majasan, J., Grondin-Perez, B., Druart, F., & Chabriat, J. P. (2021). Dimensionless approach of a polymer electrolyte membrane water electrolysis: Advanced analytical modelling. *Journal of Power Sources*, 481, 228858. <a href="https://doi.org/10.1016/j.jpowsour.2020.228858">https://doi.org/10.1016/j.jpowsour.2020.228858</a>
- [15] Guarnieri, M., Alotto, P., & Moro, F. (2015). Modeling the performance of hydrogen-oxygen unitised regenerative proton exchange membrane fuel cells for energy storage. *Journal of Power Sources*, 297, 23–32. https://doi.org/10.1016/j.jpowsour.2015.07.067
- [16] Chandesris, M., Médeau, V., Guillet, N., Chelghoum, S., Thoby, D., & Fouda-Onana, F. (2015). Membrane degradation in PEM water electrolyser: Numerical modeling and experimental evidence of the influence of temperature and current density. *International Journal of Hydrogen Energy*, 40(3), 1353–1366. https://doi.org/10.1016/j.ijhydene.2014.11.111
- [17] Springer, T. E., Zawodzinski, T. A., & Gottesfeld, S. (1991). Polymer electrolyte fuel cell. *Journal of Electrochemical Society*, *138*, 498–501. https://doi.org/10.1295/kobunshi.57.498
- [18] Xiao, H., Guo, H., Ye, F., & Ma, C. (2016). Numerical study of the dynamic response of heat and mass transfer to operation mode switching of a unitised regenerative fuel cell. *Energies*, 9(12). https://doi.org/10.3390/en9121015
- [19] Wang, L., Guo, H., Ye, F., & Ma, C. (2016). Two-dimensional simulation of mass transfer in unitized regenerative fuel cells under operation mode switching. *Energies*, 9(1), 47. https://doi.org/10.3390/en9010047
- [20] Guo, H., Wang, L. L., Yi, X. L., Ye, F., & Ma, C. F. (2018). Simulation of mode-switching methods' Effect on mass transfer in a unitized regenerative fuel cell. *Journal of Energy Engineering*, 145(1). https://doi.org/10.1061/(ASCE)EY.1943-7897.0000589
- [21] Guo, Q., Guo, H., Ye, F., & Ma, C. F. (2022). Effect of liquid water accumulation in electrolytic cell mode on start-up performance of fuel cell mode of unitised regenerative fuel cells. *Energy Conversion and Management*, 254. https://doi.org/10.1016/j.enconman.2022.115288
- [22] Guo, H., Guo, Q., Ye, F., Fang, C., Zhu, X., & Liao, Q. (2019). Three-dimensional two-phase simulation of a unitised regenerative fuel cell during mode switching from electrolytic cell to fuel cell. *Energy Conversion and Management*, 195, 989–1003. https://doi.org/10.1016/j.enconman.2019.05.069
- [23] Ferrero, D., & Santarelli, M. (2017). Investigation of a novel concept for hydrogen production by PEM water electrolysis integrated with multi-junction solar cells. *Energy Conversion and Management*, 148(2017), 16–29. <a href="https://doi.org/10.1016/j.enconman.2017.05.059">https://doi.org/10.1016/j.enconman.2017.05.059</a>
- [24] Ito, H., Maeda, T., Kato, A., Yoshida, T., & Ulleberg, Ø. (2010). gas purge for switching from electrolysis to fuel cell operation in polymer electrolyte unitized reversible fuel cells. *Journal of The Electrochemical Society*, B1072–B1080. <a href="https://doi.org/10.1149/1.3428709">https://doi.org/10.1149/1.3428709</a>
- [25] Toghyani, S., Afshari, E., Baniasadi, E., Atyabi, S. A., & Naterer, G. F. (2018). Thermal and electrochemical performance assessment of a high temperature PEM electrolyser. *Energy*, *152*, 237–246. https://doi.org/10.1016/j.energy.2018.03.140

121

Journal of Applied Science

- [26] Upadhyay, M., Kim, A., Paramanantham, S. S. S., Kim, H., Lim, D., Lee, S., Moon, S., & Lim, H. (2022). Three-dimensional CFD simulation of proton exchange membrane water electrolyser: Performance assessment under different condition. Applied Energy, 306(PA), 118016. https://doi.org/10.1016/j.apenergy.2021.118016
- [27] Sun Y., Mao L., Wang H., Liu Z., Lu S.(2022). Simulation study on magnetic field distribution of PEMFC, *Int. J. Hydrogen Energy.* 47, 33439–33452. https://doi.org/10.1016/j.ijhydene.2022.07.228.
- [28] Fan, L., Niu, Z., Zhang, G., & Jiao, K. (2018). Optimisation design of the cathode flow channel for proton exchange membrane fuel cells. *Energy Conversion and Management*, 171(May), 1813–1821. <a href="https://doi.org/10.1016/j.enconman.2018.06.111">https://doi.org/10.1016/j.enconman.2018.06.111</a>
- [29] Sarjuni, C. T. A., Lim, B. H., Majlan, E. H., Rosli, M. I., & Wong, W. Y. (2023). Analysis of fluid flow behaviour in different proton exchange membrane fuel cell flow field configurations. *Asia-Pacific Journal of Chemical Engineering*, *March*, 1–13. <a href="https://doi.org/10.1002/apj.2939">https://doi.org/10.1002/apj.2939</a>
- [30] Wu, H. W., Shih, G. J., & Chen, Y. Bin. (2018). Effect of operational parameters on transport and performance of a PEM fuel cell with the best protrusive gas diffusion layer arrangement. *Applied Energy*, 220(March), 47–58. <a href="https://doi.org/10.1016/j.apenergy.2018.03.030">https://doi.org/10.1016/j.apenergy.2018.03.030</a>
- [31] Guo, H., Song, J., Ye, F., & Fang, M. A. C. (2022). Dynamic response during mode switching of unitised regenerative fuel cells with orientational flow channels. *Renewable Energy*, *188*, 698–710. <a href="https://doi.org/10.1016/j.renene.2022.02.049">https://doi.org/10.1016/j.renene.2022.02.049</a>
- [32] Ribeirinha, P., Abdollahzadeh, M., Pereira, A., Relvas, F., Boaventura, M., & Mendes, A. (2018). High temperature PEM fuel cell integrated with a cellular membrane methanol steam reformer: Experimental and modelling. *Applied Energy*, 215(February), 659–669. https://doi.org/10.1016/j.apenergy.2018.02.029
- [33] Han, C., & Chen, Z. (2018). Study on electrochemical and mass transfer coupling characteristics of proton exchange membrane (PEM) fuel cell based on a fin-like electrode surface. *International Journal of Hydrogen Energy*, 43(16), 8026–8039. https://doi.org/10.1016/j.ijhydene.2018.02.177
- [34] Wang Z. H., Wang C. Y. (2000). Two-phase flow and transport in the interdigitated air cathode of proton exchange membrane fuel cells, *ASME Int. Mech. Eng. Congr. Expo. Proc.* 2000-S, 27–33. https://doi.org/10.1115/IMECE2000-1363.
- [35] Ferrero D., Santarelli M. (2017). Investigation of a novel concept for hydrogen production by PEM water electrolysis integrated with multi-junction solar cells, *Energy Convers. Manag.* 148, 16–29. https://doi.org/10.1016/j.enconman.2017.05.059.
- [36] Meng H. (2009). Multi-dimensional liquid water transport in the cathode of a PEM fuel cell with consideration of the micro-porous layer (MPL), *Int. J. Hydrogen Energy*. 34, 5488–5497. https://doi.org/10.1016/j.ijhydene.2009.04.067.
- [37] Dickinson E. J. F., Hinds G. (2019). The Butler-Volmer equation for Polymer Electrolyte Membrane Fuel Cell (PEMFC) Electrode Kinetics: A Critical Discussion, *J. Electrochem. Soc.* 166, F221–F231. https://doi.org/10.1149/2.0361904jes.
- [38] Chugh S., Chaudhari S., Sonkar K., Sharma A., Kapur G. S., Ramakumar S. S. V. (2020). Experimental and modelling studies of low temperature PEMFC performance, *Int. J. Hydrogen Energy*. 45, 8866–8874. https://doi.org/10.1016/j.ijhydene.2020.01.019.
- [39] Grigoriev, S. A., Millet, P., Porembsky, V. I., & Fateev, V. N. (2011). Development and preliminary testing of a unitised regenerative fuel cell based on PEM technology. *International Journal of Hydrogen Energy*, 36(6), 4164–4168. <a href="https://doi.org/10.1016/j.ijhydene.2010.07.011">https://doi.org/10.1016/j.ijhydene.2010.07.011</a>
- [40] Ito, H., Maeda, T., Nakano, A., Hwang, C. M., Ishida, M., Yokoi, N., Hasegawa, Y., Kato, A., & Yoshida, T. (2010). Influence of different gas diffusion layers on the water management of polymer electrolyte unitized reversible fuel cell. ECS Transactions, 33(1), 945–954. <a href="https://doi.org/10.1149/1.3484588">https://doi.org/10.1149/1.3484588</a>
- [41] Hasran, U. A., Pauzi, A. M., Basri, S., & A. Karim, N. (2018). Recent perspectives and crucial challenges on Unitised Regenerative Fuel Cell (URFC). *Jurnal Kejuruteraan*, 1, 37–46. https://doi.org/10.17576/jkukm-2018-si1(1)-06

Journal of Applied Science

- [42] Faustini, M., Giraud, M., Jones, D., Rozière, J., Dupont, M., Porter, T. R., Nowak, S., Bahri, M., Ersen, O., Sanchez, C., Boissière, C., Tard, C., & Peron, J. (2019). Hierarchically structured ultraporous iridium-based materials: A novel catalyst architecture for proton exchange membrane water electrolyzers. *Advanced Energy Materials*, 9(4), 1–11. https://doi.org/10.1002/aenm.201802136
- [43] Cruz, J. C., Barbosa, R., Escobar, B., Zarhri, Z., Trejo-Arroyo, D. L., Pamplona, B., & Gómez-Barba, L. (2020). Electrochemical and microstructural analysis of a modified gas diffusion layer for a PEM water electrolyser. *International Journal of Electrochemical Science*, 15, 5571–5584. <a href="https://doi.org/10.20964/2020.06.12">https://doi.org/10.20964/2020.06.12</a>
- [44] Fornaciari, J. C., Gerhardt, M. R., Zhou, J., Regmi, Y. N., Danilovic, N., Bell, A. T., & Weber, A. Z. (2020). The role of water in vapor-fed proton-exchange-membrane electrolysis. *Journal of The Electrochemical Society*, 167(10), 104508. https://doi.org/10.1149/1945-7111/ab9b09
- [45] Yuan, X. M., Guo, H., Ye, F., & Ma, C. F. (2019). Experimental study of gas purge effect on cell voltage during mode switching from electrolyser to fuel cell mode in a unitised regenerative fuel cell. *Energy Conversion and Management*, 186, 258–266. <a href="https://doi.org/10.1016/j.enconman.2019.02.067">https://doi.org/10.1016/j.enconman.2019.02.067</a>
- [46] Tang, Y., Yuan, W., Pan, M., Li, Z., Chen, G., & Li, Y. (2010). Experimental investigation of dynamic performance and transient responses of a kW-class PEM fuel cell stack under various load changes. *Applied Energy*, 87(4), 1410–1417. <a href="https://doi.org/10.1016/j.apenergy.2009.08.047">https://doi.org/10.1016/j.apenergy.2009.08.047</a>
- [47] Liu, J. X., Guo, H., Yuan, X. M., Ye, F., & Ma, C. F. (2018). Experimental investigation on two-phase flow in a unitised regenerative fuel cell during mode switching from water electrolyser to fuel cell. *International Journal of Energy Research*, 42(8), 2823–2834. https://doi.org/10.1002/er.4074
- [48] Ming, X., Guo, H., Xing, J., Ye, F., & Fang, C. (2018). Influence of operation parameters on mode switching from electrolysis cell mode to fuel cell mode in a unitised regenerative fuel cell. *Energy*, *162*, 1041–1051. <a href="https://doi.org/10.1016/j.energy.2018.08.095">https://doi.org/10.1016/j.energy.2018.08.095</a>
- [49] Li, P., Qiu, D., Peng, L., Shen, S., & Lai, X. (2022). Analysis of degradation mechanism in unitised regenerative fuel cell under the cyclic operation. *Energy Conversion and Management*, 254, 115210. https://doi.org/10.1016/j.enconman.2022.115210
- [50] Wahdame, B., Candusso, D., François, X., Harel, F., Péra, M., Hissel, D., & Kauffmann, J. (2007). Comparison between two PEM fuel cell durability tests performed at constant current and under solicitations linked to transport mission profile. 32, 4523–4536. https://doi.org/10.1016/j.ijhydene.2007.03.013
- [51] Shin, H. S., & Oh, B. S. (2020). Water transport according to temperature and current in PEM water electrolyser. *International Journal of Hydrogen Energy*, 45(1), 56–63. https://doi.org/10.1016/j.ijhydene.2019.10.209
- [52] Wang, M., Guo, H., & Ma, C. (2006). Temperature distribution on the MEA surface of a PEMFC with serpentine channel flow bed. *Journal of Power Sources*, 157, 181–187. <a href="https://doi.org/10.1016/j.jpowsour.2005.08.012">https://doi.org/10.1016/j.jpowsour.2005.08.012</a>
- [53] Xiao, H., Dai, L. Y., Song, J., Guo, H., Ye, F., & Ma, C. F. (2018). Dynamic response of a unitised regenerative fuel cell under various ways of mode switching. *International Journal of Energy Research*, 42(3), 1328–1337. https://doi.org/10.1002/er.3934
- [54] Meng, H. (2007). Numerical investigation of transient responses of a PEM fuel cell using a two-phase non-isothermal mixed-domain model. *Journal of Power Sources*, 171, 738–746. <a href="https://doi.org/10.1016/j.jpowsour.2007.06.029">https://doi.org/10.1016/j.jpowsour.2007.06.029</a>
- [55] Liu, J. X., Guo, H., Yuan, X. M., Ye, F., & Ma, C. F. (2019). Effect of mode switching on the temperature and heat flux in a unitised regenerative fuel cell. *International Journal of Hydrogen Energy*, 44(30), 15926–15932. https://doi.org/10.1016/j.ijhydene.2018.05.113
- [56] Guo, Q., Guo, H., Ye, F., Ma, C. F., Liao, Q., & Zhu, X. (2019). Heat and mass transfer in a unitised regenerative fuel cell during mode switching. *International Journal of Energy Research*, 43(7), 2678–2693. https://doi.org/10.1002/er.4319

- [57] Bhosale A. C., Meenakshi S., Ghosh P. C. (2017). Root cause analysis of the degradation in a unitized regenerative fuel cell, *J. Power Sources*. 343 275–283. https://doi.org/10.1016/j.jpowsour.2017.01.060.
- [58] Speder, J., Zana, A., Spanos, I., Kirkensgaard, J. J. K., Mortensen, K., Hanzlik, M., & Arenz, M. (2014). Comparative degradation study of carbon supported proton exchange membrane fuel cell electrocatalysts e The influence of the platinum to carbon ratio on the degradation rate. *Journal of Power Sources*, 261, 14—22. https://doi.org/10.1016/j.jpowsour.2014.03.039
- [59] Regmi, Y. N., Peng, X., Fornaciari, J. C., Wei, M., Myers, D. J., Weber, A. Z., & Danilovic, N. (2020). A low temperature unitised regenerative fuel cell realising 60% round trip efficiency and 10,000 cycles of durability for energy storage applications. *Energy & Environmental Science*. 3(7), 2096-2105. https://doi.org/10.1039/C9EE03626A

